INVESTIGATING THE BINDING INTERACTIONS AND STABILITY OF MODIFICATIONS OF FURANOCOUMARINS TO CYCLIN DEPENDENT KINASE 4 USING MOLECULAR DOCKING AND MD SIMULATIONS

Abstract

The cell-cycle regulator, CDK4 (Cyclin Dependent Kinase 4) is found to be hyperactive in cancer cells leading to unrestricted cell division. The established antagonists of CDK4 are associated with various toxicities in humans. Furanocoumarins produce chemotherapeutic effects in a variety of cancer cells including direct inhibition of CDK4. Thus, designing furanocoumarin derived compounds and evaluating their inhibitory behaviour against CDK4 is aimed to improve efficiencies of known inhibitors. In this study, we carried out 8 modifications by substituting the acetonide ring of a furanocoumarin oxypeucedanin hydrate acetonide to different positions of another furanocoumarin notopterol. Following this, we performed docking studies of these eight modifications to the ligand binding zone of CDK4, along with a well known inhibitor of the protein, abemaciclib which was used as the control. Thereafter, rank_1 and rank_2 of the best scored ligand- modification_7, along with abemaciclib were progressed to subsequent MD (Molecular Dynamics) simulations. The modifications bound to CDK4 with appreciable negative binding energies, modification_7 being the highest scored ligand, as obtained from molecular docking calculations. Modification_7 was reasonably stable inside the ligand binding pocket of CDK4 as obtained from MD simulations. This study contributes insights on the inhibitory tendencies of natural compound like molecules against cell-cycle related proteins, hence guiding experimentalists in inventing better inhibitors.

Keywords: CDK4; molecular docking; molecular dynamics.

Authors

Srutishree Sarma
CMML–Catalysis and Molecular Modelling Lab
Department of Chemical Sciences
Tezpur University
Napaam, Sonitpur, Assam, India.

Nishant Biswakarma
CMML–Catalysis and Molecular Modelling Lab
Department of Chemical Sciences
Tezpur University
Napaam, Sonitpur, Assam, India.

Moumita Basumatary
CMML–Catalysis and Molecular Modelling Lab
Department of Chemical Sciences
Tezpur University
Napaam, Sonitpur, Assam, India.

Nand Kishor Gour
CMML–Catalysis and Molecular Modelling Lab
Department of Chemical Sciences
Tezpur University
Napaam, Sonitpur, Assam, India.

Ramesh Chandra Deka
CMML–Catalysis and Molecular Modelling Lab
Department of Chemical Sciences
Tezpur University
Napaam, Sonitpur, Assam, India.
ramesh@tezu.ernet.in

I. INTRODUCTION

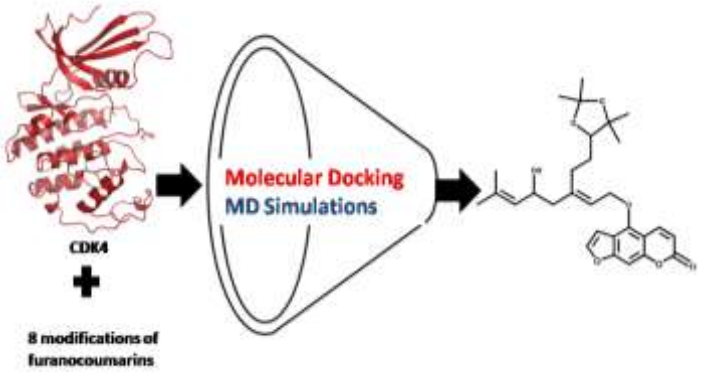

The constant processes of cell-cycle and division are regulated dominantly by a group of enzymes called Cyclin Dependent Kinases [1]. Cyclin Dependent Kinase 4 (CDK4) is one such type of enzyme that controls the entry into the S phase from the G1 phase of cell cycle [2]. This kinase causes phosphorylation of Rb (retinoblastoma) which then releases certain transcription factors engaged in the transcription of genes related to the phase transition [1,3]. Uncontrolled upregulation of CDK4 and the associated regulatory enzyme Cyclin D is found to be responsible for elevated cell division, subsequently causing cancer [4]. As a consequence, CDK4 is thought to be an appropriate target in chemotherapeutics.

The available antagonists of CDK4 like palbocilcib, abemaciclib and ribociclib lead to various adverse effects like diarrhea, increased creatinine, nausea, reduced white blood cells etc [5, 6]. Hence, the quest for harmless drugs continues. Furanocoumarins are phytochemicals constituting a furan ring linked to a coumarin unit and are dominantly present in grapefruits, carrots, etc [7, 8]. Among the diverse beneficial roles of these class of compounds is their potential to induce anti cancerous effects in diverse human cancer cells [9]. They are reported to reduce cell division by arresting the cell –cycle in different stages [10]. Furanocoumarins like psoralen and bergamottin lead to G1 stage arrest by down regulating CDK4 along with Cyclin D [11, 12]. One furanocoumarin, Isoimperatorin was found to inhibit CDK4 in prostate cancer [13]. Psoralidin, a derivative of psoralen promoted the arrest of cell division in the G1 stage wherein the arrest was associated with inhibition of CDK4 [14]. Acharya et al. conducted docking studies of furanocoumarins onto proteins associated with breast cancer [15].

In this work, we carried out 8 modifications by substituting the acetonide ring of a furanocoumarin named oxypeucedanin hydrate acetonide (CID_70697919) to different positions of the alkoxy chain of notopterol (CID_5320227) (Figure 1). We then investigated the inhibitory powers of these 8 modifications along with abemaciclib, an FDA (Food and Drug Administration) approved inhibitor of CDK which was used as a control; against CDK4 using molecular docking and molecular dynamics simulations [16]. This study is believed to provide insights on the potential of natural compound like molecules to inhibit cell-cycle related proteins and thus help experimentalists in developing better inhibitors targeting CDK4.

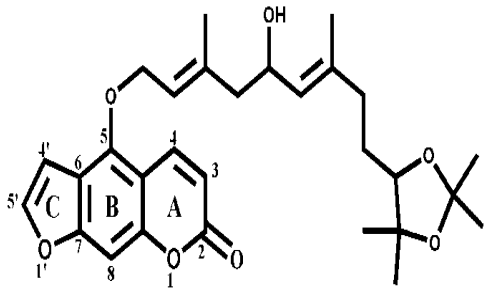

modification_1

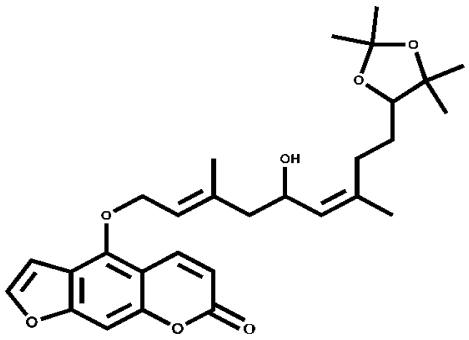

modification_2

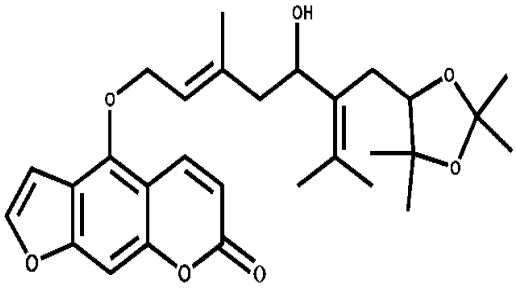

modification_3

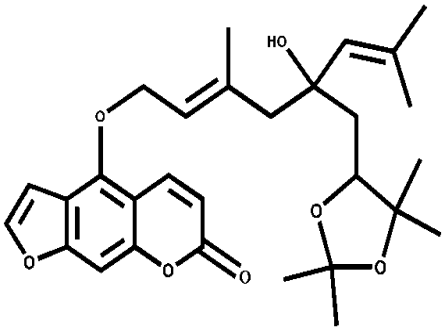

modification_4

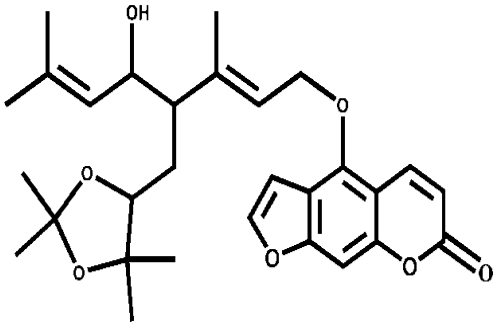

modification_5

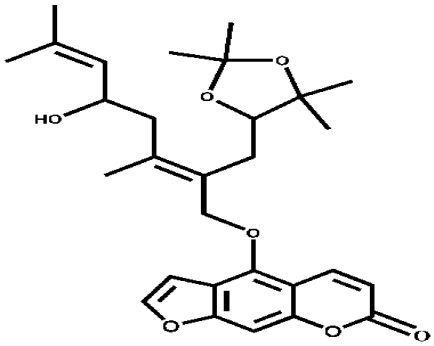

modification_6

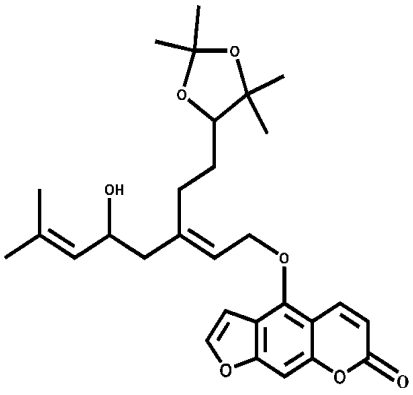

modification_7

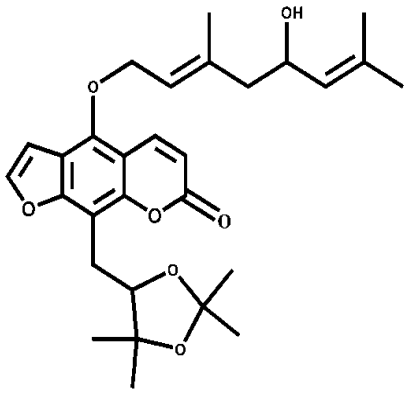

modification_8

Figure 1: Structures of Modified Furanocoumarins Considered for this Study

II. MATERIALS AND METHODS

1. **Geometry Optimization of compounds:** Geometry optimization of compounds must be carried out before beginning any investigation in order to derive the lowest energy structures wherein atoms are aligned in the most stable form [17]. Structures of each compound were constructed using Gauss View followed by subsequent geometry optimization utilizing Gaussian 09 software [18] and B3LYP/6-31+G(d,p) level of theory [19].

2. **Retrieval of CDK4 Structure:** We used the active CDK4 PDB (Protein Data Bank) structure provided by Shafiq et al., as the experimental X-ray structure of the protein in its active orientation was not available in the scientific literature [20]. The core of the protein structure developed by the group was retrieved from the X-ray structure of CDK4 in its inactive conformation (pdb ID: 2W96) whereas the active states of the α-C helix and activation loop were derived through homology modeling upon an active structure of CDK2 (Cyclin Dependent Kinase 2) with RCSB PDB (Research Collaboratory for Structural Bioinformatics Protein Data Bank) ID: 1FIN. This hybrid form of CDK4 along with the geometry optimized compounds was considered for subsequent docking studies.

3. **Molecular Docking:** Molecular docking of the optimized compounds was carried out employing the free available AutoDock 4.2 software wherein the 9 ligands including the 8 modification along with the control were allowed to approach the ATP (Adenosine Tri-phosphate)-binding active zone of CDK4 [21]. This technique is helpful in evaluating the binding interactions and docking energies of ligands to large receptor proteins [22]. Grid box was set surrounding the CDK4 ATP binding zone containing important catalytic residues like Val96, His95, Lys35 etc. No. of grid points present along each dimension was 48 with a spacing of 0.5 Å between consecutive points. The Lamarckian genetic algorithm was used as the search method to find out the stable lowest energy conformations of the ligands. Top 10 lowest energy modes were procured from docking calculations for each of the compounds. The most potent modified ligand along with abemaciclib was considered for further investigation.

4. **Molecular Dynamics Simulations:** Rank-1 and rank-2 conformations of the most potent modification along with the rank-1 conformation of abemaciclib were selected as initial inputs for MD simulations employing GROMACS (GROningen MAchine for Chemical Simulations) 2022 program and CHARMM (Chemistry at Harvard Macromolecular Mechanics) 36 force field [23, 24]. Each ligand\CDK4 complex was placed in the centre of a dodecahedron and subsequently the box was solvated with TIP3P (Transferrable Intermolecular Potential with 3 points) water [25].

   Ligand parameters were generated using the CGennFF (CHARMM General Force Field) server which is suitable for the CHARMM force field [26]. In order to get rid of steric repulsions and irregular geometries, energy minimizations were carried out for each system within 50000 steps applying the steepest decent algorithm wherein the solvated systems acquired potential energy of around -10^5 (kJ/mol) order. Subsequently, the systems were put through the NVT (constant particles, volumn and temperature) equilibration step wherein the temperature was adapted around 300K within 500ps

utilizing the velocity-rescaling coupling procedure [27]. Following this step, the system was carried through an NPT (constant particles, pressure and temperature) equilibration process which equilibrated the pressure near 1atm. Finally, the systems were subjected to production mdrun step for 100ns for each of the three systems. Constrains were applied to bonds engaging H atoms utilizing LINCS (LInear Constraint Solver) algorithm [28]. PME (Particle Mesh Ewald) was used to compute long range electrostatics [29]. Verlet cut-off procedure was used to truncate nonbonded forces at 1.2nm [30]. The GROMACS module gmxrms was used to evaluate MD trajectories and PyMOL package was utilized to analyze interactions [31].

5. **MM-PBSA Binding Free Energy:** MM-PBSA (Molecular Mechanics Poisson-Boltzman Surface Area) is a method that can be utilized to calculate binding free energies of small ligand molecules to macromolecular targets. The GROMACS module g_mmpbsa was implemented to investigate free energies of binding of the ligands to CDK4 active region from the output MD trajectories [32]. The general formula for calculation of binding free energy is represented as:

$$\Delta G_{binding} = G_{complex} - G_{protein} - G_{ligand} \quad (1)$$

Here the first, second and third terms depict the corresponding Gibb's free energies of protein/ligand complex, free protein and ligand. Every free energy component is a summation of vacuum molecular mechanical energy and non-polar and polar solvation energy [33]. In the work, MM-PBSA binding free energies of each ligand/receptor complex was computed from the 100ns MD simulation output trajectory as a mean of 101 frames where frames were taken after every 1000ps gap. Poisson-Boltzman equation was utilized to estimate polar energy of solvation and nonpolar energy of solvation was computed with the help of the SASA only model.

III. RESULTS AND DISCUSSION

1. **Geometry Optimization**: Structures of the 8 modifications and abemaciclib were brought to their lowest energy structures through geometry optimization utilizing Gaussian 09. The optimized geometries of all molecules are illustrated in Figure 2.

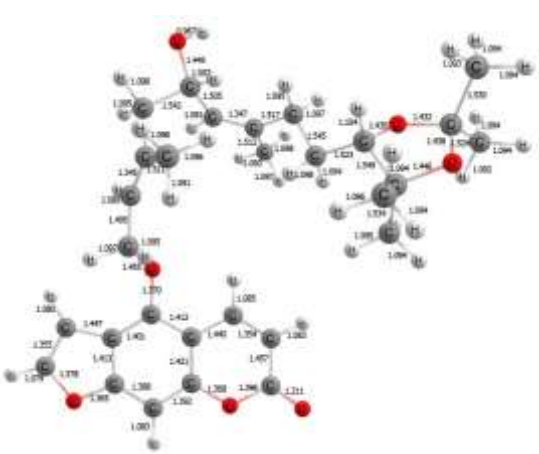

modification_1

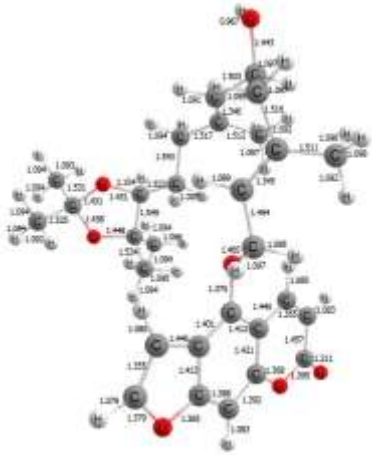

modification_2

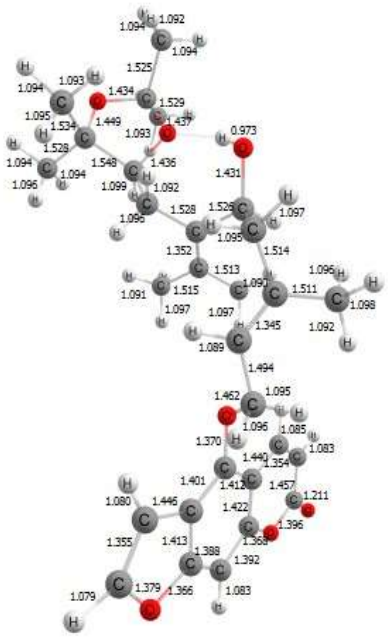

modification_3

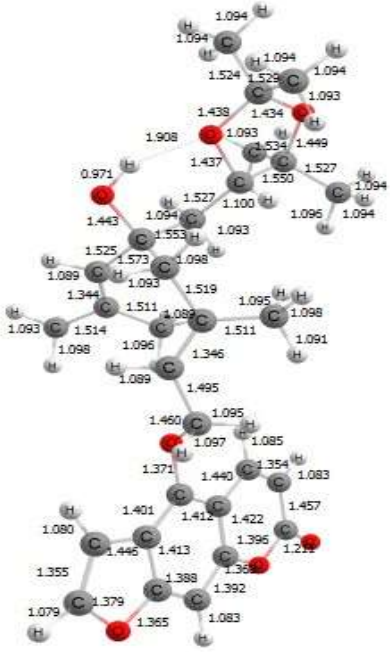

modification_4

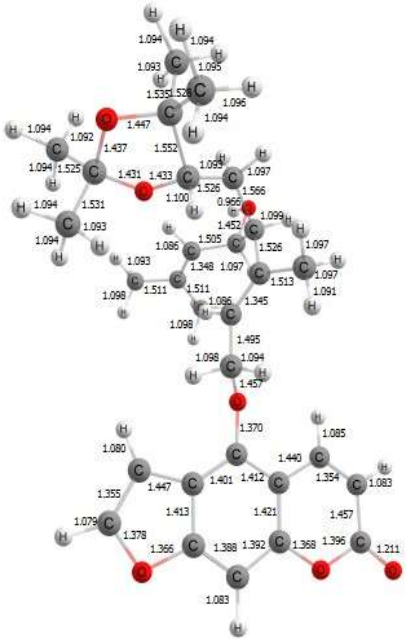

modification_5

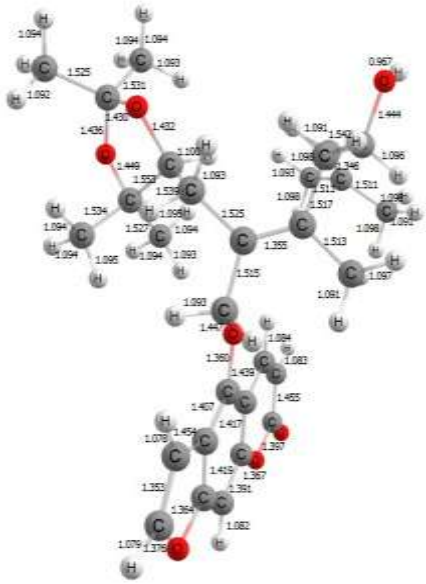

modificatin_6

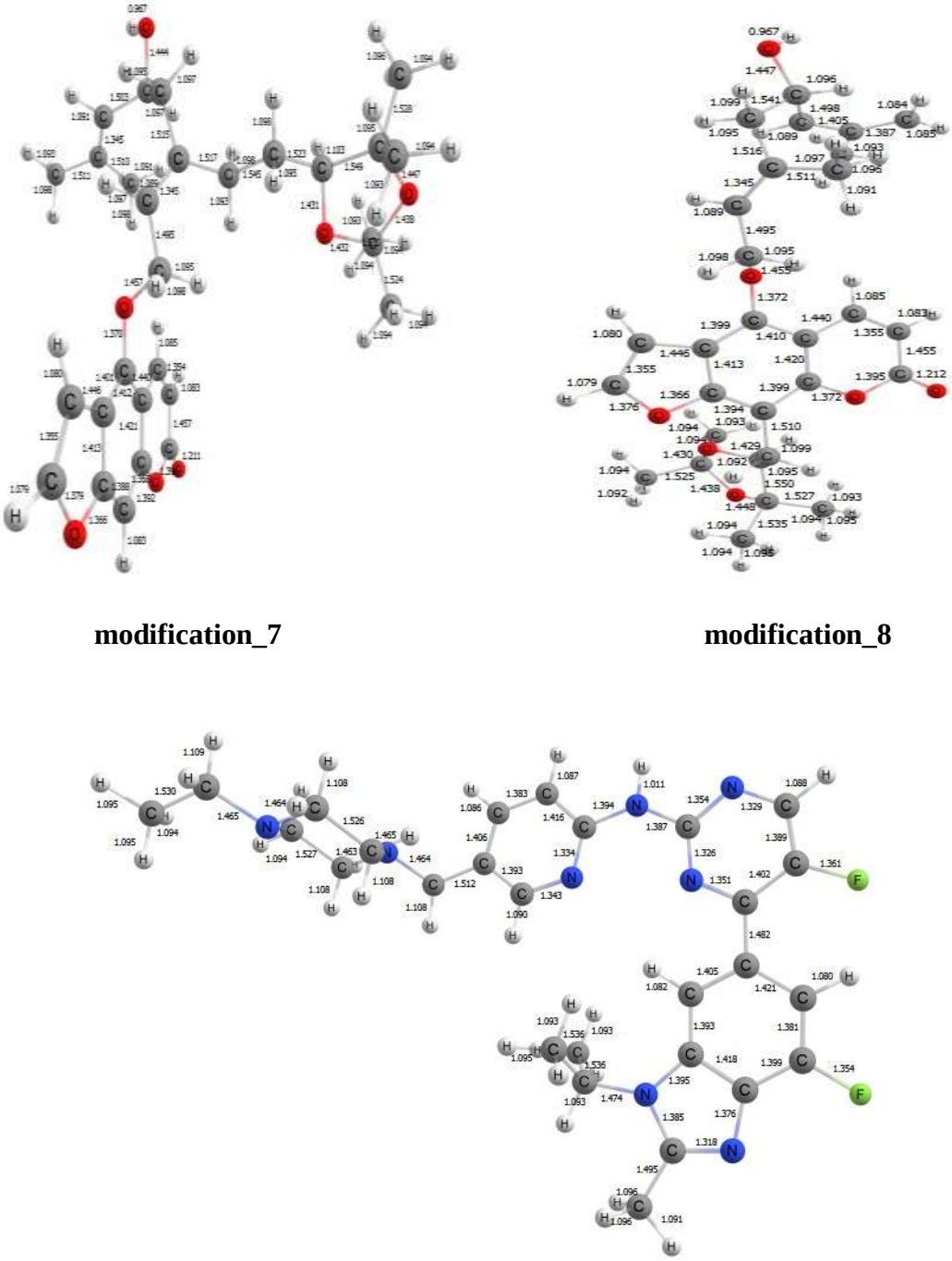

modification_7 **modification_8**

Abemaciclib

Figure 2: Optimized Structures of Modified Furanocoumarins and Control Ligand

2. **Molecular Docking:** Molecular docking of the 8 modifications and abemaciclib were carried out where ligands were allowed to approach into the ATP-binding region of CDK4 (Figure 3) and corresponding best scores of the ligands are shown in Table 1.

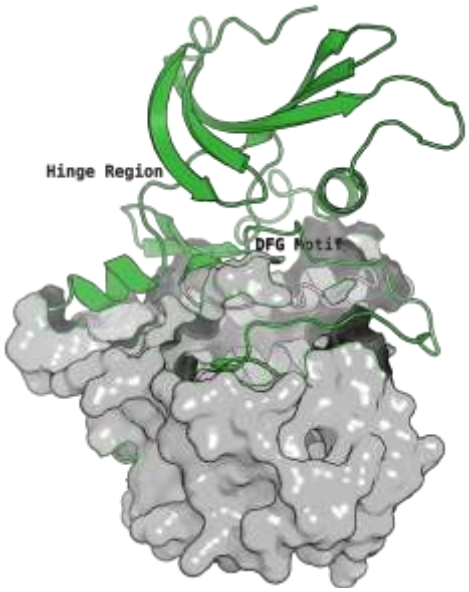

Figure 3: Active Catalytic ATP-Binding Region of CDK4 Shown in Green Cartoon, Rest of the Protein Shown as Grey Surface.

Table 1: Best Docked Scores/Binding Energies of Modified Ligands and Control to CDK4

Ligands	Binding energy (kcal/mol)
modification_1	-8.6
modification_2	-8.15
modification_3	-8.67
modification_4	-8.9
modification_5	-8.02
modification_6	-8.56
modification_7	-9.36
modification_8	-8.65
abemaciclib	-8.36

As inferred from the table, all the modifications interacted with the active site of CDK4 with fairly negative scores of more than -8 kcal/mol. Modification_1, modification_3, modification_4, modification_6, modification_7 and modification_8 had scores more negative than the control drug abemaciclib, the one with the most negative score being modification_7.

All the modifications engaged through hydrogen bonds in the CDK4 ligand binding site with amino acids like Asp158, Val96, Glu144, Lys35, Phe159, Gly18, Asp99, His95, Val14, Lys142 etc as obtained from studying the interactions from their top-scored poses (Figure 4). Different types of hydrogen bonds like conventional, pi-donor and carbon were present between the ligands and protein receptor. Modification_7

with the most negative energy formed two H-bonds with Gly18 and Val96; Val96 being a principal residue in the active ligand binding region of CDK4 [34]. In addition, a pi-anion type of attractive association was observed in the presence of modification_7. Interestingly, modification_8 formed three conventional hydrogen bonds with Val14, His95 and Asp99; however one unfavorable acceptor-acceptor repulsive contact was detected in the system, which might be the cause behind its lower binding score than modification_7 wherein only two H-bonds were present.

The control ligand abemaciclib was also seen associating with conventional and pi-donor hydrogen bonds with similar residues like Gly18, Asp99, and Asp158 etc. Furthermore, various hydrophobic contacts like pi-alkyl, pi-sigma, pi-pi stalked etc. were present between the compounds and CDK4 augmenting the hydrogen bonds. Thus, the modifications occupied the binding pocket with contacts which were analogous to the control drug abemaciclib. Hence, from the docking energy analysis modification_7 was shortlisted along with the control for succeeding MD studies.

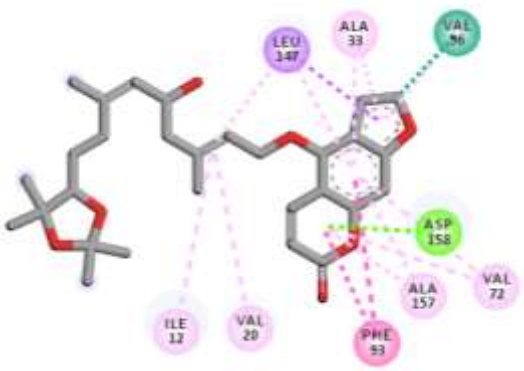

modification_1

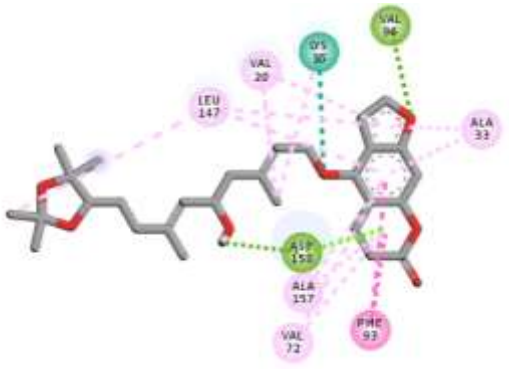

modification_2

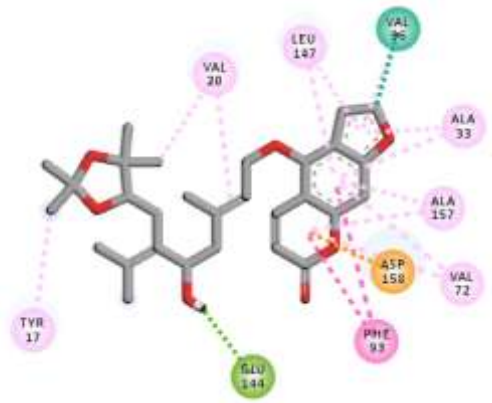

modification_3

modification_4

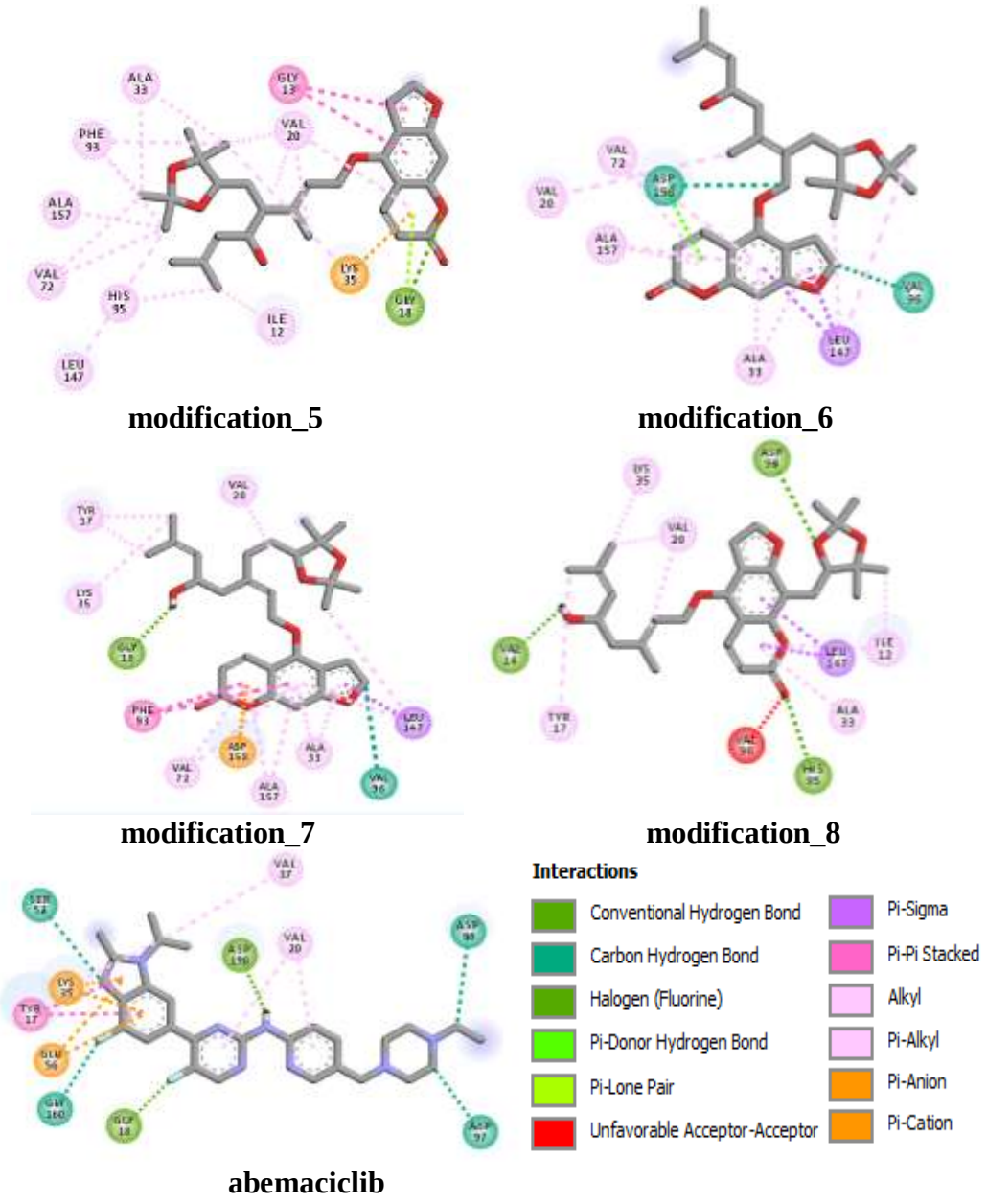

Figure 4: Interactions of Ligands with the Active Region of CDK4

3. Molecular Dynamics Simulations

- **RMSD Analysis:** MD simulations of the rank_1 and rank_2 conformations of the best docked modification i.e. modification_7 along with rank_1 conformation of the control ligand abemaciclib in complex with CDK4 receptor were performed for 100ns in order to explore their stabilities in the ligand binding site of CDK4. RMSD (Root Mean Square Deviation) study was conducted to procure protein backbone behaviour during 100ns simulations. RMSD profile of CDK4 backbone in its complex with modification_7 (rank_1) was almost analogous to the backbone deviation in complex with the control (Figure 5). The deviations were also considerably reduced compared

to bare CDK4. Values were sustained around 0.45 nm during the last 20ns. Thus from the RMSD graph, it can be observed that CDK4 backbone in its complex with modification_7 did not undergo any unusual structural deviation and maintained a stable from all over 100ns. Modification_7 along with the control stayed inside the active zone of CDK4 for the entire 100ns. Moreover, ligand RMSD values of the highest scored conformation (rank_1) of the modification were considerably less in relation to those of the control abemaciclib (Figure 6). Rank_2 of modification_7 however was substantially unstable with elevated RMSD values reaching upto 2nm, hence rank_2/CDK4 system was removed from further analysis. All graphs, figures and any mention of modification_7 thus refer to the top scored rank_1 conformation of the ligand.

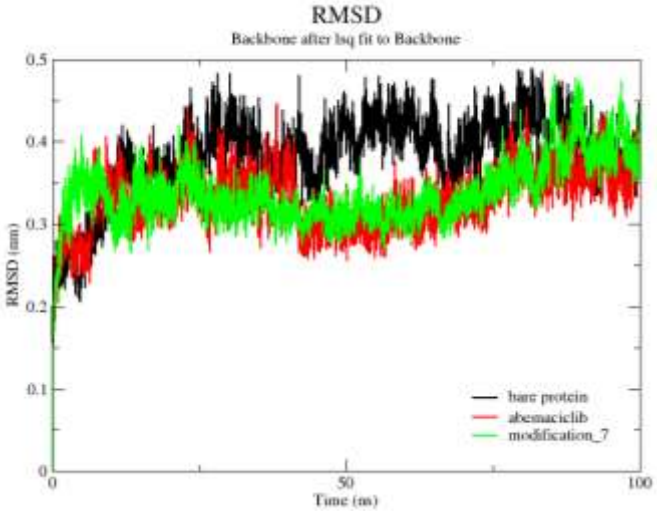

Figure 5: RMSD Graphs of Bare CDK4 Backbone and When Associated with Ligands

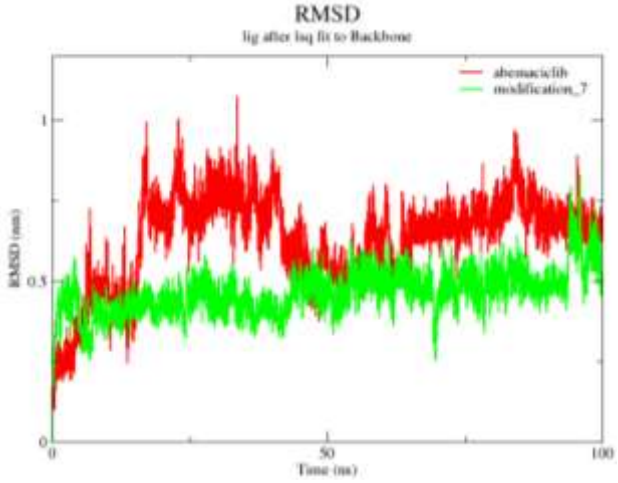

Figure 6: RMSD Graphs of Ligands with Respect to CDK4 Backbone

- **Rg Analysis:** Rg (Radius of Gyration) study was performed to estimate the variation in protein fold during 100ns. Rg of CDK4 in complex with modification_7 resembled to that in complex with the control and was also preserved close to the apo protein

mostly during the last 20ns (Figure 7). Rg values of the enzyme were sustained near 2.17 in modification_7/CDK4 system.

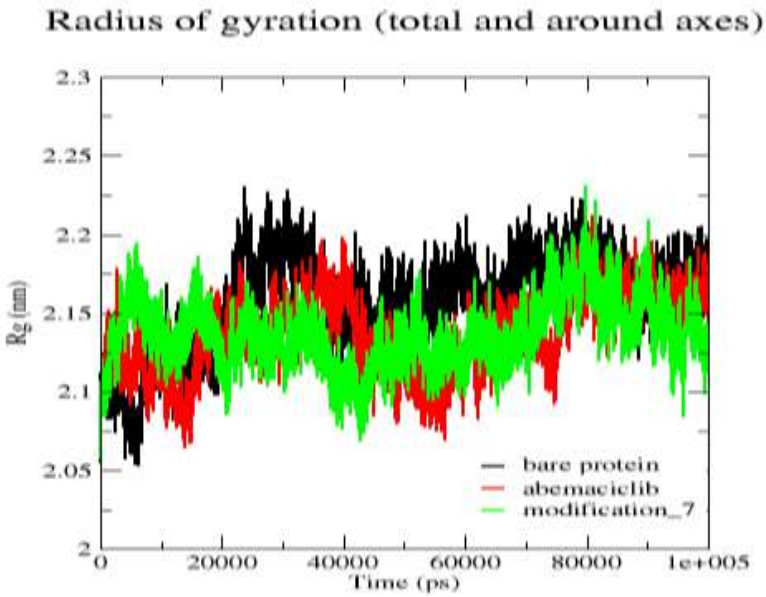

Figure 7: Radius of Gyration of Bare CDK4 and When Associated to Ligands

- **RMSF Analysis:** Study of fluctuations of CDK4 backbone atoms was done through RMSF (Root Mean Square Fluctuation) analysis. Interestingly, backbone fluctuations of modification_7 intensified in most areas of the enzyme compared to the control encompassing core catalytic regions like the hinge region (Phe93-Val96) and DFG motif (Asp158-Gly160) of CDK4 (Figure 8). Moreover, the DFG segment of the backbone on incorporation of modification_7 showed a slight increase in RMSF compared to the bare protein.

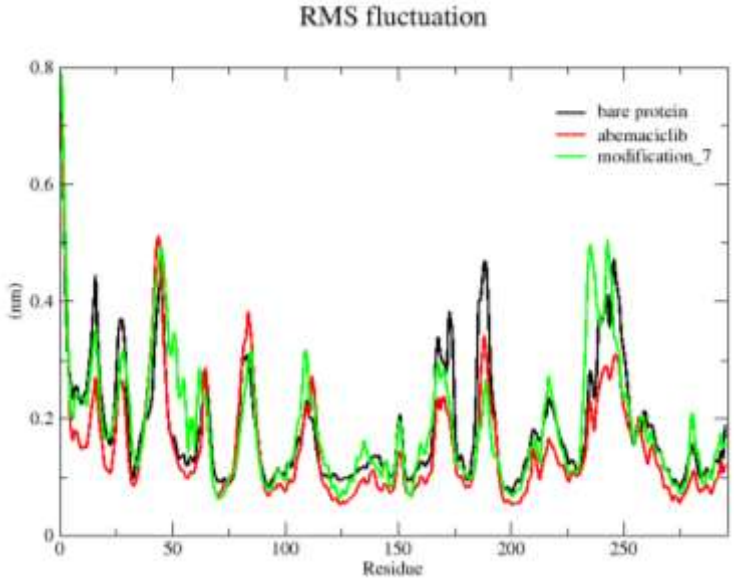

Figure 8: RMSF Graphs of Bare CDK4 Backbone and When Associated to Ligands

- **SASA Analysis:** Evaluation of the amount of surface area of the protein which is within reach by the solvent can be done through SASA or Solvent Accessible Surface Area analysis. It also provides an idea about the changes in the protein form on associating with a ligand [35]. SASA of modification_7/CDK4 adduct was stable without any major deviation over the duration of 100ns. Values were less compared to the adduct formed with abemaciclib control and was conserved in the vicinity of the bare protein. Thus, CDK4 on incorporating modification_7 resulted in a more compact form than the other two systems as derived from reduced SASA (Figure 9).

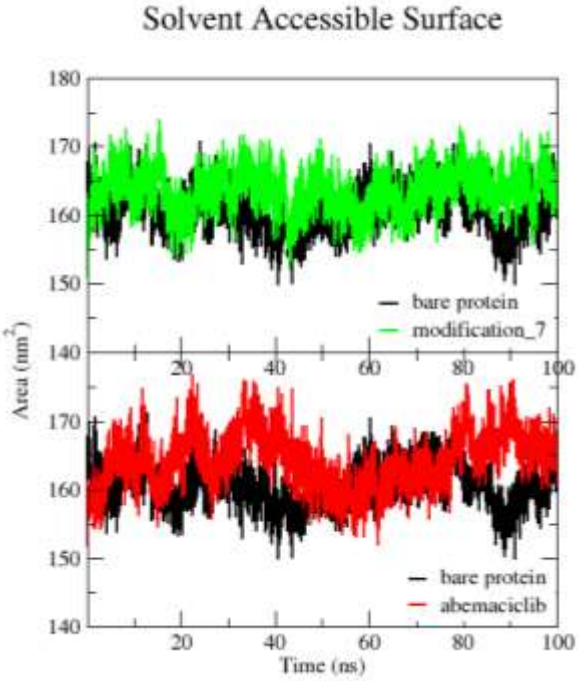

Figure 9: SASA Graphs of Bare CDK4 and in Complex with the Ligands

- **Hydrogen Bond Analysis:** Modification_7 along with the control ligand formed extensive hydrogen bonds inside the active ATP-binding region of CDK4. Interactions between the ligands and CDK4 were observed at every 10ns interval of the 100ns simulation trajectory. Table 2 and figure 10 depict the important hydrogen bonds present in the bimolecular systems. Lys35 of CDK4 was found to be diligently occupied with H-bonds in presence of the modification as well as the control engaging the carbonyl oxygen (O7) of the coumarin fragment of modification_7 and nitrogen atoms of pyrimidine (N4) and pyridine rings (N6) of abemaciclib respectively. Occupancy on associations with abemaciclib control (72.72% and 90.90%) was apparently more as compared to the modified furanocoumarin (54.54%). However, modification_7 formed additional bonds with important residues in the active region. Two bonds were formed involving Asp158 of DFG (Aspartic acid-Phenylalanine-Glycin) segment and the carbonyl oxygen (O7) with 36.36% occupancy. Carbon atom adjacent to the oxygen of the furan ring (C24) donated one hydrogen bond to the backbone oxygen of Glu94 which is a prime residue in the hinge region of the catalytic pocket, retaining 45.45% possession [35]. Thus it can be

observed that the modification formed hydrogen bonds which resembled to some extent the contacts formed by the control inhibitor abemaciclib.

Table 2: Occupancy Percentages of Hydrogen Bonds Formed between Ligands and CDK4 during Entire 100ns Simulation

Ligand	Donor-Acceptor	Occupancy (%)
modification_7	CA (Asp158)-O7(Lig)	36.36
	NZ (Lys35)-O7(lig)	54.54
	CE (Lys35)- O7(lig)	18.18
	N (Asp158)-O7 (lig)	36.36
	C24 (lig)-O (Val96)	18.18
	C24 (lig)-O (Glu94)	45.45
	C4 (lig)-O (Glu144)	18.18
	O1 (lig)- O (Glu144)	27.27
	O1 (lig)-O (Val14)	18.18
	O1 (lig)-OD1 (Asn145)	18.18
abemaciclib	CB (Ser52)-F2 (lig)	18.18
	NZ (Lys35)-N4 (lig)	90.9
	NZ (Lys35)-N6 (lig)	72.72
	CE (Lys35)-N6 (lig)	18.18
	C18 (lig)-O (Val14)	27.27
	C19 (lig)-O (Ile12)	36.36
	N5 (lig)-O (Tyr17)	18.18
	C21 (lig)-O (Val96)	18.18
	C23 (lig)-O (Asp97)	18.18

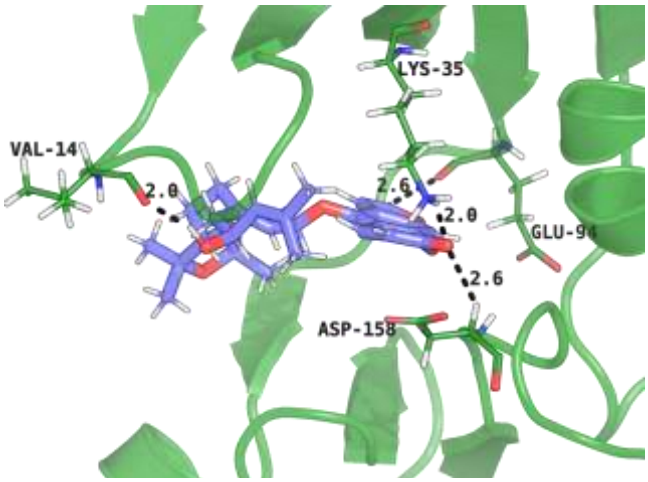

modification_7/CDK4 complex

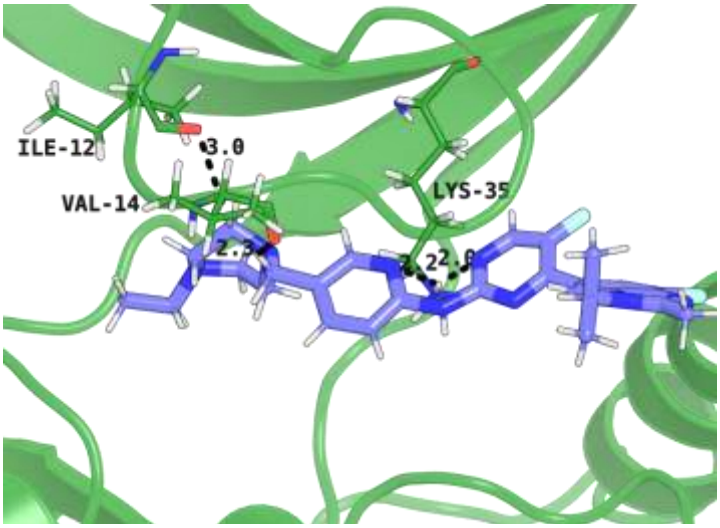

abemaciclib/CDK4 complex

Figure 10: Stable Hydrogen Bonds Present between Ligands and the Active Area of CDK4

Both the modification and the control remained incorporated inside the ligand binding zone during the entire 100ns. However, there were minor conformational changes in the ligands over the duration of the simulation time. Owing to the more elongated structure of abemaciclib, its conformational changes were more distinct between 0, 50 and 100ns compared to modification_7 (figure 11). This might be the cause behind more RMSD values of the control as compared to the modification.

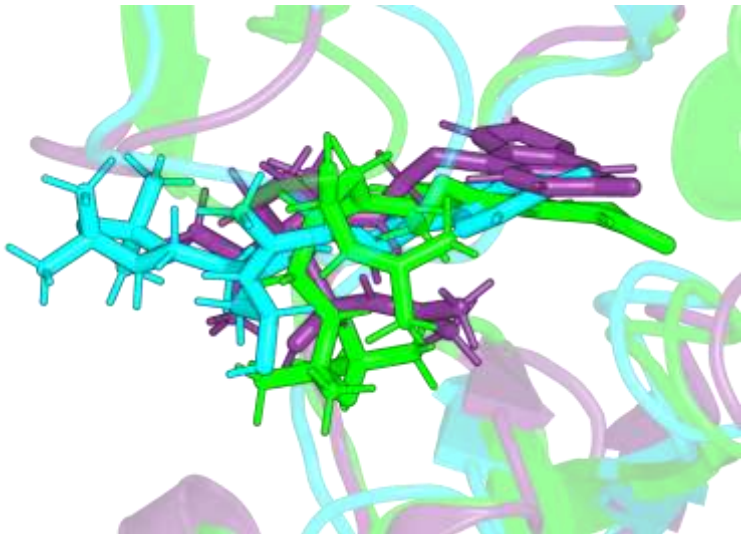

modification_7/CDK4 complex

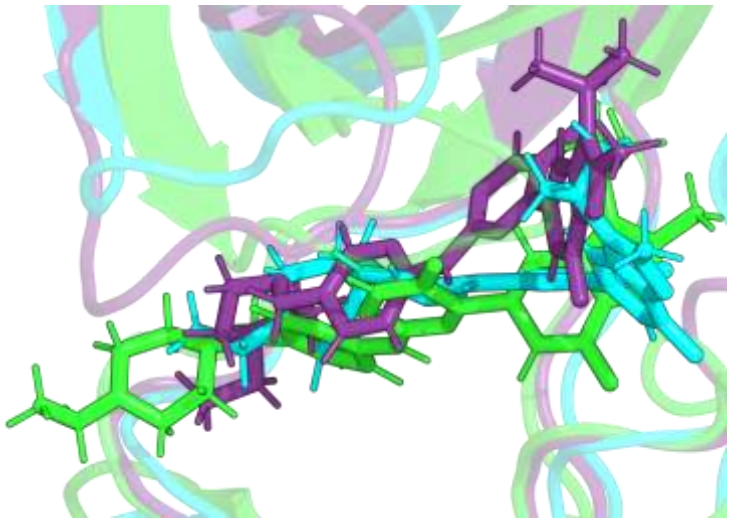

abemaciclib/CDK4 complex

Figure 11: Poses Of Ligands at 0ns (Green), 50ns (Cyan) and 100ns (Violet) Simulation Time

4. **MM-PBSA Free Energy of Binding:** Energies of binding of the modification and the control to CDK4 were determined using the MM-PBSA free energy estimation method for entire 100ns trajectory. Table 3 lists ΔG_Bind (binding free energy), together with ΔE_vdW (van der Waals energy), ΔE_Ele (electrostatic energy), ΔE_Sol_Nonpolar (non-polar solvation energy) and ΔE_Sol_Polar (polar solvation energy) contributions. Modification_7 exhibited appreciable negative energy in relation to the control abemaciclib.

   Dominant contributing component was the van der Waals energy which was very much negative compared to abemaciclib\CDK4 system. Presence of extra hydrophobic interactions like alkyl-alkyl, pi-alkyl and pi-pi interactions in the modification_7\CDK4 system might be the source behind this result. The van der Waals contribution was augmented by a lower value of the positive polar solvation energy in contrast to the control system.

Table 3: MM-PBSA free energy of binding (kcal/mol) of modified ligand and control to CDK4

Ligands	ΔG_Bind	ΔE_vdW	ΔE_Ele	ΔE_Sol_Polar	ΔE_Sol_Nonpolar
abemaciclib	- 9.38 ± 0.58	-36.87 ± 0.53	-15.05 ± 0.59	47.79 ± 0.99	-5.22 ± 0.07
modification_7	-21.17 ± 0.51	-46.71± 0.47	-10.73 ± 0.52	41.85 ± 0.74	-5.58 ± 0.04

IV. CONCLUSIONS

In this work, 8 modifications derived from the natural furanocoumarins notopterol and oxypeucedanin hydrate acetonide were designed and targeted against the cell cycle

protein CDK4 using in-silico processes of protein\ligand docking, molecular dynamics simulations and MM-PBSA binding energy estimations. As obtained from docking analysis, modification_7 interacted with CDK4 with the highest docked score which was also higher than the control ligand abemaciclib. Thus, modification_7 along with abemaciclib were chosen for succeeding MD simulations. The modification was substantially more stable than the control as obtained from the reduced ligand RMSD of the former. Both the ligands hydrogen bonded with principal catalytic residues like Lys35. Modification_7 exhibited high negative MM-PBSA binding energy in relation to the control drug abemaciclib specifying its stability in the catalytic region of CDK4. This finding bestows novel insights into the quest for developing better targets for cell-cycle related proteins and thus is believed to aid succeeding investigations in this field.

REFERENCES

[1] M. Peyressatre, C. Prével, M. Pellerano, and M. C. Morris, “Targeting cyclin-dependent kinases in human cancers: from small molecules to peptide inhibitors,” Cancers,2015.
[2] S. J. Baker, P. I. Poulikakos, H. Y. Irie, S. Parekh, and E. P. Reddy, “CDK4: a master regulator of the cell cycle and its role in cancer,” Genes Cancer, vol. 13(21), 2022.
[3] M. Malumbres and M. Barbacid, M. “Cell cycle, CDKs and cancer: a changing paradigm,” Nat. Rev. Cancer, vol. 9(3), pp. 153-166, 2009.
[4] R. Roskoski Jr, “Cyclin-dependent protein kinase inhibitors including Palbociclib as anticancer drugs,” Pharmacol. Res., vol. 107, pp. 249-275, 2016.
[5] Q. Du, X. Guo, M. Wang, Y. Li, X. Sun, and Q. Li, “The application and prospect of CDK4/6 inhibitors in malignant solid tumors, ”J. Hematol. Oncol., vol. 13, pp. 1-12, 2020.
[6] F. Schettini, I. De Santo, C. G. Rea, P. De Placido, L. Formisano, M. Giuliano et al., “CDK 4/6 inhibitors as single agent in advanced solid tumors,” Front. Oncol., vol. 8(608), 2018.
[7] R. Bruni, D. Barreca, M. Protti, V. Brighenti, L. Righetti, L. Ancesch et al., “Botanical sources, chemistry, analysis, and biological activity of furanocoumarins of pharmaceutical interest,” Molecules, vol. 24(11), 2019.
[8] M. M. Melough, E. Cho, and O. K. Chun, “Furocoumarins: a review of biochemical activities, dietary sources and intake, and potential health risks,” Food Chem. Toxicol., vol. 113, pp. 99-107, 2018.
[9] W. L. Hung, J. H. Suh, and Y. Wang, “Chemistry and health effects of furanocoumarins in grapefruit,” J Food Drug Anal, vol. 25(1), pp. 71-83, 2017.
[10] T. J. Kang, S. Y. Lee, R. P. Singh, R. Agarwal, and D. S. Yim, “Anti-tumor activity of oxypeucedanin from Ostericum koreanum against human prostate carcinoma DU145 cells,” Acta Oncol, vol. 48(6), pp. 895-900, 2009.
[11] O. Vetrichelvan, P. Gorjala, O. Goodman Jr, and R. Mitra, “Bergamottin a CYP3A inhibitor found in grapefruit juice inhibits prostate cancer cell growth by downregulating androgen receptor signaling and promoting G0/G1 cell cycle block and apoptosis,” PLoS One., vol. 16(9), 2021.
[12] C. Wu, Z. Sun, Y. Ye, X. Han, X. Song, and S. Liu, “Psoralen inhibits bone metastasis of breast cancer in mice,” Fitoterapia, vol. 91, pp. 205-210, 2013.
[13] J. H. Kang, S. K. Lee, and D. S. Yim, “Effect of isoimperatorin on the proliferation of prostate cancer cell line DU145 cells,” *Biomol. Ther.*, vol. 13(3), pp. 185-189, 2005.
[14] T. Gulappa, R. S. Reddy, S. Suman, A. M. Nyakeriga, and C. Damodaran, “Molecular interplay between cdk4 and p21 dictates G0/G1 cell cycle arrest in prostate cancer cells,” Cancer Lett., vol. 337(2), pp. 177-183, 2013.
[15] R. Acharya, S. Chacko, P. Bose, A. Lapenna, and S. P. Pattanayak, “Structure based multitargeted molecular docking analysis of selected furanocoumarins against breast cancer,” Sci. Rep., vol. 9(1), pp. 1-13, 2019.
[16] Y. Wu, Y. Zhang, H. Pi, and Y. Sheng, “Current therapeutic progress of CDK4/6 inhibitors in breast cancer,” Cancer Manag. Res., vol. 12, 2020.
[17] E. G. Lewars, Computational Chemistry: Introduction to the Theory and Apllications of Molecular and Quantum Mechanics, 2nd ed., Springer, 2011.

[18] M. J. Frisch, G. W. Trucks, H. B. Schlegel, G. E. Scuseria, M. A. Robb, J. Cheeseman et al., Gaussian 09, revision D.01; Gaussian, Inc: Wallingford, CT, 2009.
[19] P. J. Stephens, F. J. Devlin, C. F. Chabalowski, and M. J. Frisch, "Ab initio calculation of vibrational absorption and circular dichroism spectra using density functional force fields" J. Phys. Chem., vol. 98(45), pp. 11623-11527, 1994.
[20] M. I. Shafiq, T. Steinbrecher, and R. Schmid, "Fascaplysin as a specific inhibitor for CDK4: insights from molecular modelling" PLoS One, vol. 7(8):e42612, 2012.
[21] G. M. Morris, R. Huey, W. Lindstrom, M. F. Sanner, R. K. Belew, D. S. Goodsell, and A. J. Olson, "AutoDock4 and AutoDockTools4: automated docking with selective receptor flexibility" J. Comput. Chem., vol. 30(16), pp. 2785-2791, 2009.
[22] S. Cosconati, S. Forli, A. L. Perryman, R. Harris, D. S. Goodsell, and A. J. Olson, "Virtual screening with AutoDock: theory and practice," Expert Opin Drug Discov, vol. 5(6), pp. 597-607, 2010.
[23] M. J. Abraham, T. Murtola, R. Schulz, S. Páll, J. C. Smith, B. Hess, and E. Lindahl, "GROMACS: High performance molecular simulations through multi-level parallelism from laptops to supercomputers," Softwarex, vol. 1-2, pp. 19-25, 2015.
[24] R. B. Best, X. Zhu, J. Shim, P. E. Lopes, J. Mittal, M. Feig, A. D. MacKerell Jr, " Optimization of the additive CHARMM all-atom protein force field targeting improved sampling of the backbone ϕ, ψ and side-chain $\chi 1$ and $\chi 2$ dihedral angles," J. Chem. Theory Comput., vol. 8(9), pp. 3257-3273, 2012.
[25] A. D. MacKerell Jr, D. Bashford, M. L. D. R. Bellott, R. L. Dunbrack Jr, J. D. Evanseck, M. J. Field et al., "All-atom empirical potential for molecular modeling and dynamics studies of proteins" J. Phys. Chem. *B*, vol. 102(18), pp. 3586-3616, 1998.
[26] K. Vanommeslaeghe, E. Hatcher, C. Acharya, S. Kundu, S. Zhong, J. Shim et al., "CHARMM general force field: A force field for drug-like molecules compatible with the CHARMM all-atom additive biological force fields," J Comput Chem, vol. 31(4), pp. 671-690,2010.
[27] G. Bussi, D. Donadio, and M. Parrinello, "Canonical sampling through velocity rescaling," J. Chem. Phys., vol. 126(1), 2007.
[28] H. J. Berendsen, J. V. Postma, W. F. Van Gunsteren, A. R. H. J. DiNola, and J. R. Haak, "Molecular dynamics with coupling to an external bath," J. Chem. Phys., vol. 81(8), pp. 3684-3690, 1984.
[29] B. Hess, H. Bekker, H. J. Berendsen, and J. G. Fraaije, "LINCS: a linear constraint solver for molecular simulations," J Comput Chem, vol. 18(12), pp. 1463-1472, 1997.
[30] T. Darden, D. York, and L. Pedersen, "Particle mesh Ewald: An N· log (N) method for Ewald sums in large systems," J. Chem. Phys., vol. 98(12), pp. 10089-10092, 1993.
[31] S. Páll, and B. Hess, "A flexible algorithm for calculating pair interactions on SIMD architectures," Comput Phys Commun, vol. 184(12), pp. 2641-2650, 2013.
[32] Schrödinger Release 2023-4: The PyMOL Molecular Graphics System; Version 2.5.5; Schrödinger, LLC: New York, 2023. https://pymol.org/2/ (accessed 2023-08-20)
[33] R. Kumari, and R. Kumar, "Open Source Drug Discovery Consortium; Lynn, A. g_mmpbsa□ A GROMACS tool for high-throughput MM-PBSA calculations,"J Chem Inf Model, vol. 54(7), pp. 1951-1962, 2014.
[34] P. A. Kollman, I. Massova, C. Reyes, B. Kuhn, S. Huo, L. Chong et al., "Calculating structures and free energies of complex molecules: combining molecular mechanics and continuum models," Acc. Chem. Res., vol. 33(12), pp. 889-897, 2000.
[35] N. M. P. Susanti, S. Damayanti, R. E. Kartasasmita, and D. H. Tjahjono, "A search for cyclin-dependent kinase 4/6 inhibitors by pharmacophore-based virtual screening, molecular docking, and molecular dynamic simulations," Int. J. Mol. Sci., vol. 22(24), 2021.
[36] E. Durham, B. Dorr, N. Woetzel, R. Staritzbichler, and J. Meiler, "Solvent accessible surface area approximations for rapid and accurate protein structure prediction," J Mol Model, vol. 15, pp. 1093-1108,2009.

